

# **Eight-Port MIMO Antenna System for 2.6 GHz LTE Cellular Communications**

**Naser O. Parchin<sup>1, \*</sup>, Haleh J. Basherlou<sup>2</sup>, Yasir I. A. Al-Yasir<sup>1</sup>,  
Ahmed M. Abdulkhaleq<sup>1</sup>, Raed A. Abd-Alhameed<sup>1</sup>, and Peter Excell<sup>3</sup>**

**Abstract**—In this paper, an eight-port antenna array operating in the 2.6 GHz band (2550–2650 MHz) for a multi-input multi-output (MIMO) mobile terminal is presented. The configuration of the design is composed of four pairs of low-profile dual-polarized slot antennas that are symmetrically placed at the corners of a mobile-phone mainboard. Each antenna pair consists of miniaturized petal-shaped slot resonators fed by two independent microstrip-feeding lines, thus facilitating radiation pattern and polarization diversity: when acting together, they facilitate multi-channel MIMO operation. The design offers good isolation, dualpolarization and full radiation coverage in a smartphone sized package. A low-cost FR-4 dielectric ( $\epsilon = 4.4$ ,  $\delta = 0.02$ , and  $h = 0.8$  mm) with a dimension of  $75 \times 150$  mm<sup>2</sup> is used as the PCB substrate. The characteristics of the smartphone antenna are examined using both simulations and measurements.

## **1. INTRODUCTION**

MIMO systems with multiple-antenna units at both transmitter and receiver sides can take advantage of multipath components sufficiently to enhance the performance of wireless systems [1]. As MIMO technology can significantly enhance the capacity of the system and resist multipath fading, it has become a hot spot in the field of wireless communication [2, 3]. MIMO technology requires that all antenna radiators work simultaneously. It has been employed in current handheld mobile devices and become a promising technology to be used in future user equipment [4, 5].

The standard MIMO technology employs two or four elements. However, in order to achieve a better MIMO performance, higher data rate, and more stable signal quality, a high number of antenna radiators are required to be implemented in fifth-generation (5G) equipment [6]. Due to the available RF circuit and test system of 2.6 GHz communication, long-term evolution (LTE) technology is becoming the default for future cellular communications, and it has drawn many interests recently [7, 8]. To realize MIMO operation for smartphones, multi-antenna design can be used for having polarization and pattern diversity for reliable communication with sufficient mutual coupling [9, 10]. In this study, an eight-element MIMO array is proposed for possible 5G smartphones.

Low profile and wideband MIMO antennas with sufficient isolation are suitable to be used in mobile applications [11, 12]. Among various MIMO antennas, printed antennas such as monopole, slot, and planar inverted F-Antenna (PIFA) antennas are more suitable due to their compact profile, low cost, easy integration, and manufacturability [13–15]. Recently, several MIMO antenna designs have been reported for smartphones at sub 6 GHz operation band [16–19]. However, these smartphone antennas either use single-fed/single-polarized radiators or employ uniplanar structures occupying large spaces of

---

*Received 17 November 2019, Accepted 11 January 2020, Scheduled 24 January 2020*

\* Corresponding author: Naser Ojaroudi Parchin (N.OjaroudiParchin@Bradford.ac.uk).

<sup>1</sup> Faculty of Engineering and Informatics, University of Bradford, Bradford, United Kingdom. <sup>2</sup> Bradford College, Bradford, Bradford, United Kingdom. <sup>3</sup> Department of Engineering, Wrexham Glyndwr University, Wrexham LL11 2AW, UK.

PCB leading to increasing the system complexity. We introduce here a design of four-element/Eight-port MIMO smartphone antenna with low-profile antenna elements providing polarization and pattern diversity function. The designed antenna operates at 2.6 GHz, a frequency band of cellular networks.

The configuration of the designed antenna array comprises four pairs of dual-polarized petal-shaped slot antenna radiators placed at different corners of the mainboard. In order to reduce the size of radiation elements, petal-ring slot antenna elements have been employed in the configuration of the presented MIMO antenna design. By exciting the antenna elements from two microstrip feed lines, two orthogonally polarized waves are generated. The proposed MIMO antenna is designed on an FR-4 dielectric with properties of  $\epsilon = 4.4$ ,  $\delta = 0.02$ , and  $h = 0.8$  mm. The design not only generates dual-polarizations but also provides the required full radiation coverage. A prototype of the proposed design is fabricated, and its  $S$ -parameters are measured. The *CST Microwave Studio* software is used to investigate the characteristics and performance of the MIMO design [20].

## 2. PERFORMANCE OF THE DOUBLE-PORT PETAL-SHAPED SLOT ANTENNA

Figure 1(a) depicts the schematic of the designed antenna. As shown, the design is composed of a petal-ring slot radiator differently fed by a pair of 50-Ohm rectangular microstrip-lines. It is designed on a 0.8 mm FR4 dielectric and operates at 2.6 GHz. The parameter values of the designs are specified in Table 1.

Figure 1(b) illustrates the  $S$ -parameter results of the dual-port designed petal-ring slot antenna. As shown, the antenna element exhibits good reflection coefficient ( $S_{11}/S_{22}$ ) in the frequency band of 2.5–2.7 GHz. In addition, the antenna offers a sufficient transmission coefficient ( $S_{21}/S_{12}$ ) function, better than  $-10$  dB, without additional decoupling structure. Figure 2 illustrates the antenna  $S_{11}$  characteristic of varying design parameters of the petal-ring slot resonator including  $L$  (size of the slot-ring),  $L_2$  (width

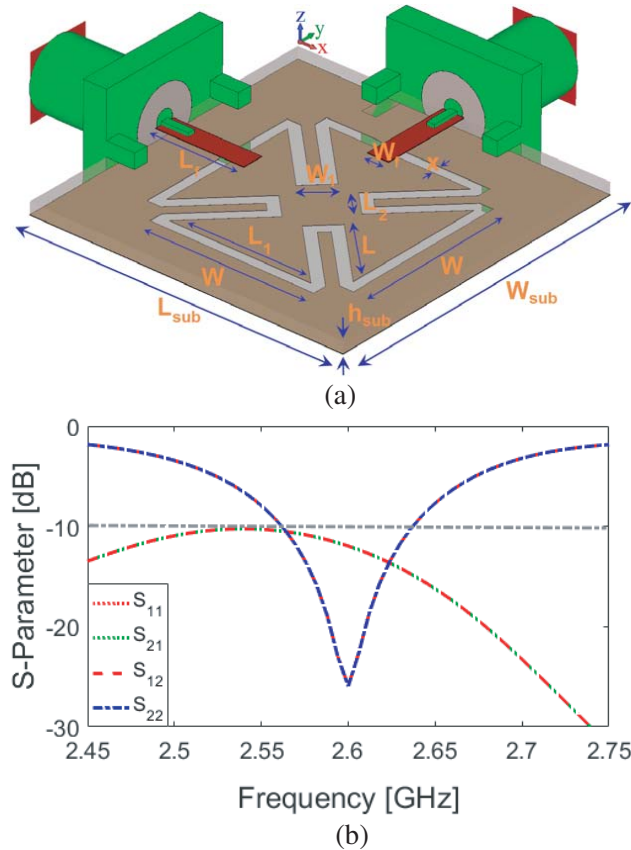


**Figure 1.** (a) Proposed antenna configuration and (b) its simulated  $S$ -parameters.

**Table 1.** The optimized values of the design parameters.

Parameter	$W_{sub}$	$L_{sub}$	$h_{sub} = h_x$	$W_f$	$L_f$	$W$
Value (mm)	22	22	0.8	1.5	6.25	11.5
Parameter	$W_1$	$L$	$L_1$	$L_2$	$W_X$	$L_X$
Value (mm)	2.25	11.5	9.9	2.25	150	75

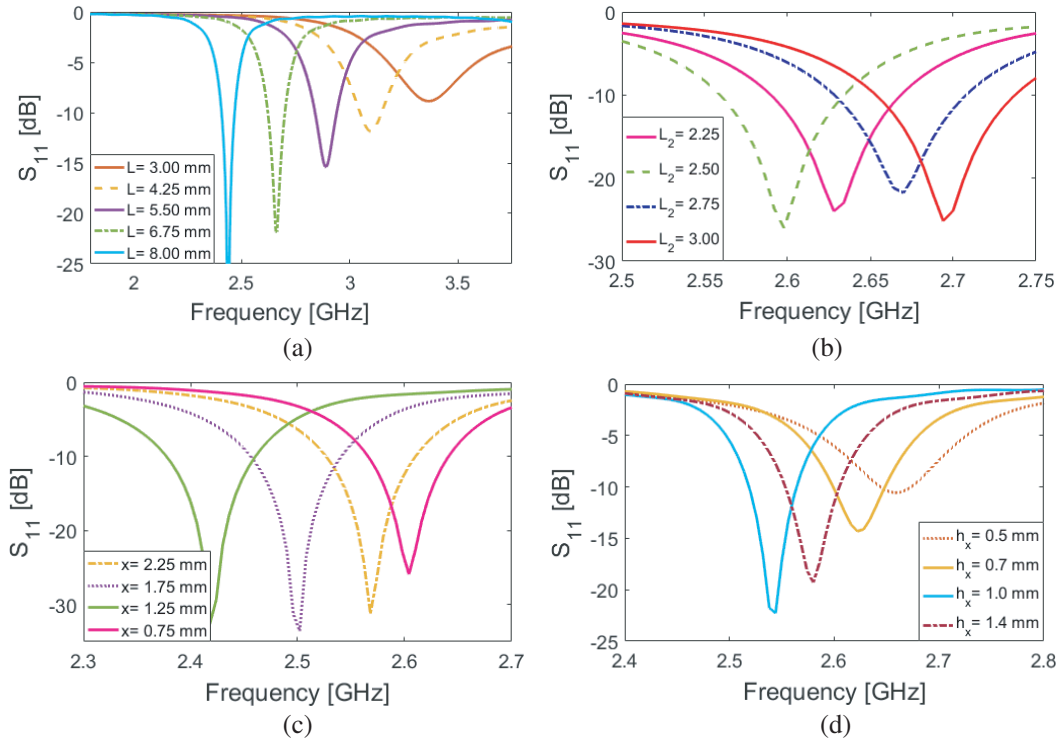


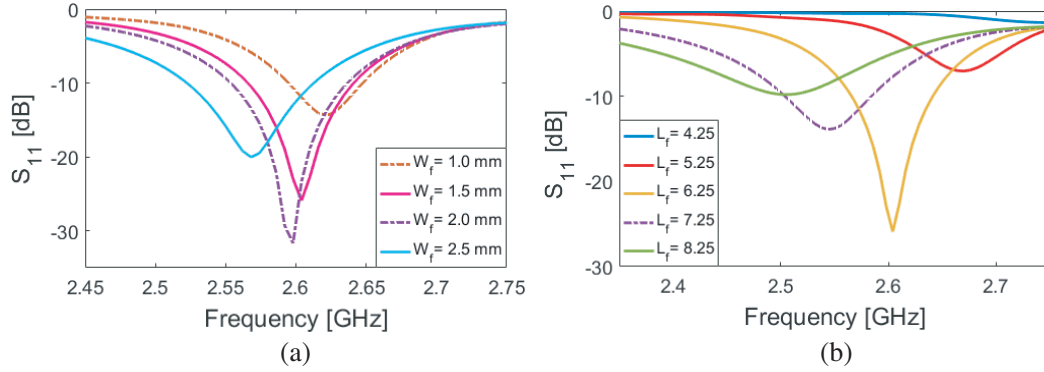
**Figure 2.**  $S_{11}$  results for the different values of (a)  $L$ , (b)  $L_2$ , (c)  $x$ , and (d)  $h_x$ .

of the petal arm), (c)  $x$  (width of the ring), and (d)  $h_x$  (thickness of the substrate). As can be observed, the antenna frequency response is very flexible to be tuned to lower or upper frequencies [21, 22]. Its impedance matching can also be affected by changing the parameter values.

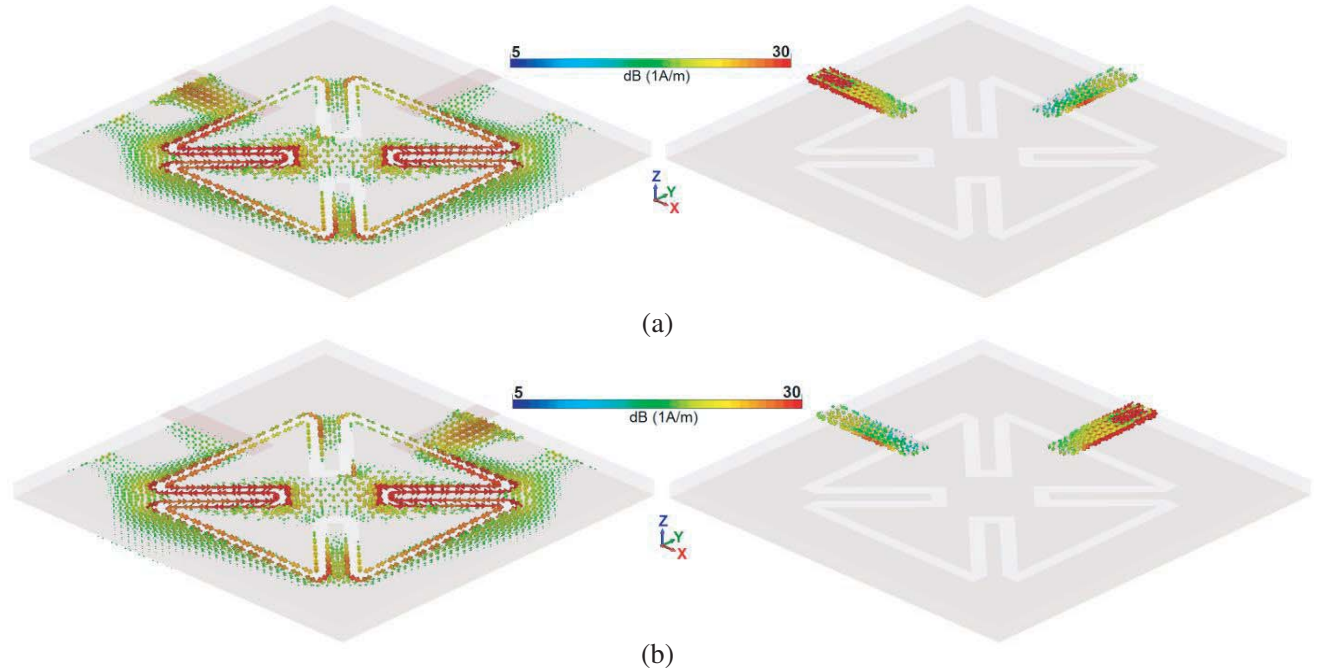
Apart from the petal-ring slot, the dimension of the feed-lines in the top layer could also affect the operation frequency and impedance bandwidth of the antenna. Figures 3(a) and (b) plot the  $S_{11}$  results of the antenna for different sizes of  $W_f$  (width of feed-line) and  $L_f$  (length of the feed-line). As can be observed, changing the width and length of the microstrip feed-line not only affects the impedance matching of the antenna but also can tune the operation frequency of the design [23, 24].

Figure 4 depicts the current densities in the back and top surface layers of the petal-shaped slot antenna at the resonance frequency of 2.6 GHz for different feeding ports. It can be observed that the maximum current distributions are more concentrated around the petal-ring slot radiators. In other words, the employed slot ring appears very active with high current densities. In addition, due to the dual-polarization function of the design, for different feeding ports, the currents flow in the opposite directions [25]. Furthermore, as shown, in the top layer, the current flows are mainly distributed around the employed rectangular feed-lines.

3D radiation patterns at 2.6 GHz for different polarizations are illustrated in Figure 5. It can be seen that the antenna provides good dual-polarization characteristics with a 90° difference and similar radiation pattern performances with 3.15 dB IEEE gain. A prototype sample of the design is fabricated, as illustrated in Figure 6.



**Figure 3.**  $S_{11}$  results for the different values of (a)  $W_f$  and (b)  $L_f$ .



**Figure 4.** Variation of surface currents in the top and bottom layers at 2.6 GHz from feeding port (a) 1 and (b) 2.

Figure 7 shows the measured and simulated  $S$ -parameters ( $S_{11}$  &  $S_{21}$ ) of the design. It is found that the prototype works properly, and a good agreement with the simulation is observed for the presented antenna. As shown, an impedance bandwidth ( $S_{11} \leq -10$  dB) of 2.55–2.66 GHz is achieved, although for  $S_{11} \leq -6$  dB, the antenna impedance bandwidth is more. In addition, as shown, the mutual-coupling function ( $S_{21}/S_{12}$ ) of the design is less than  $-10$  dB which makes it suitable for dual-polarization applications.

### 3. CHARACTERISTICS OF THE $8 \times 8$ MIMO SMARTPHONE ANTENNA

Figure 8 illustrates the configuration of the designed MIMO smartphone antenna. As shown, it comprises four pairs of dual-polarized loop radiators placed at different corners of the mainboard. It is designed on FR-4 material with a thickness of  $h_x = 0.8$  mm. As can be observed, the 50-Ohm microstrip feeding technique feeds the antenna elements. The proposed MIMO antenna array is implemented on a low-cost FR4 with dimension of  $75 \times 150$  mm<sup>2</sup> and a standard size of the smartphone mainboard.

Figure 9 depicts the  $S$  parameters of the designed smartphone antenna. As shown, the antenna

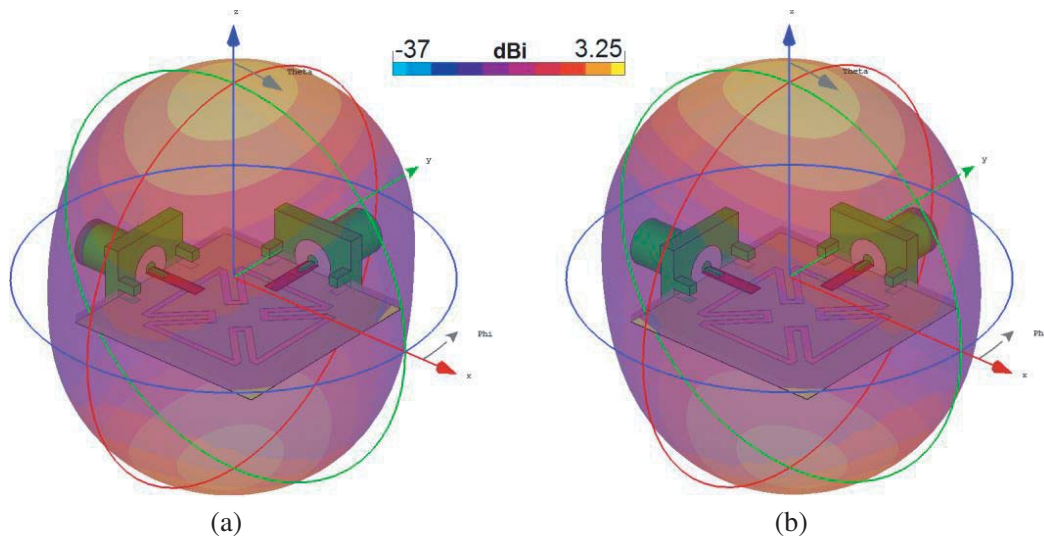


Figure 5. Transparent radiation patterns at 2.6 GHz from feeding port (a) 1 and (b) 2.

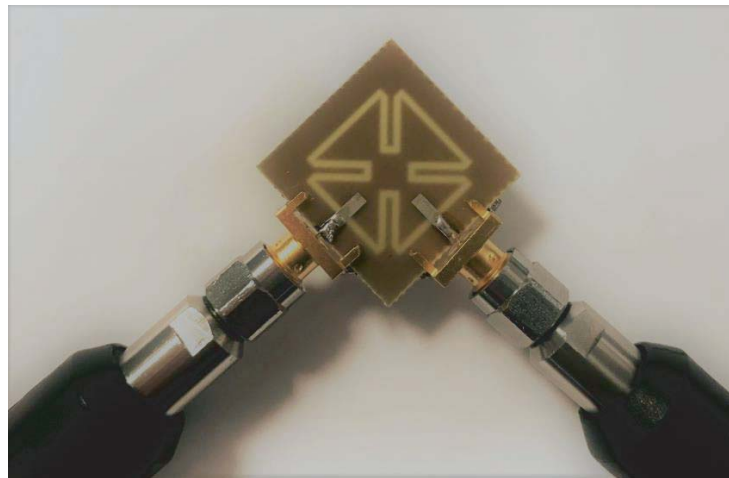


Figure 6. Fabricated dual-polarized petal-shaped antenna.

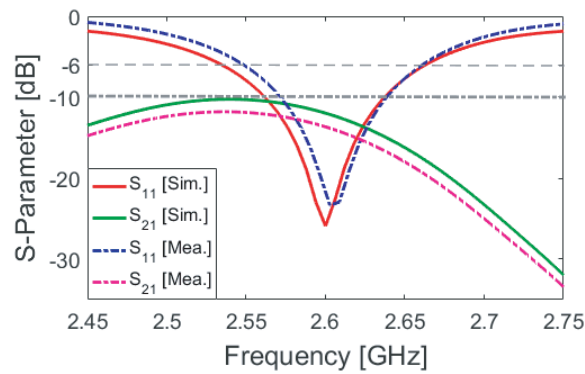
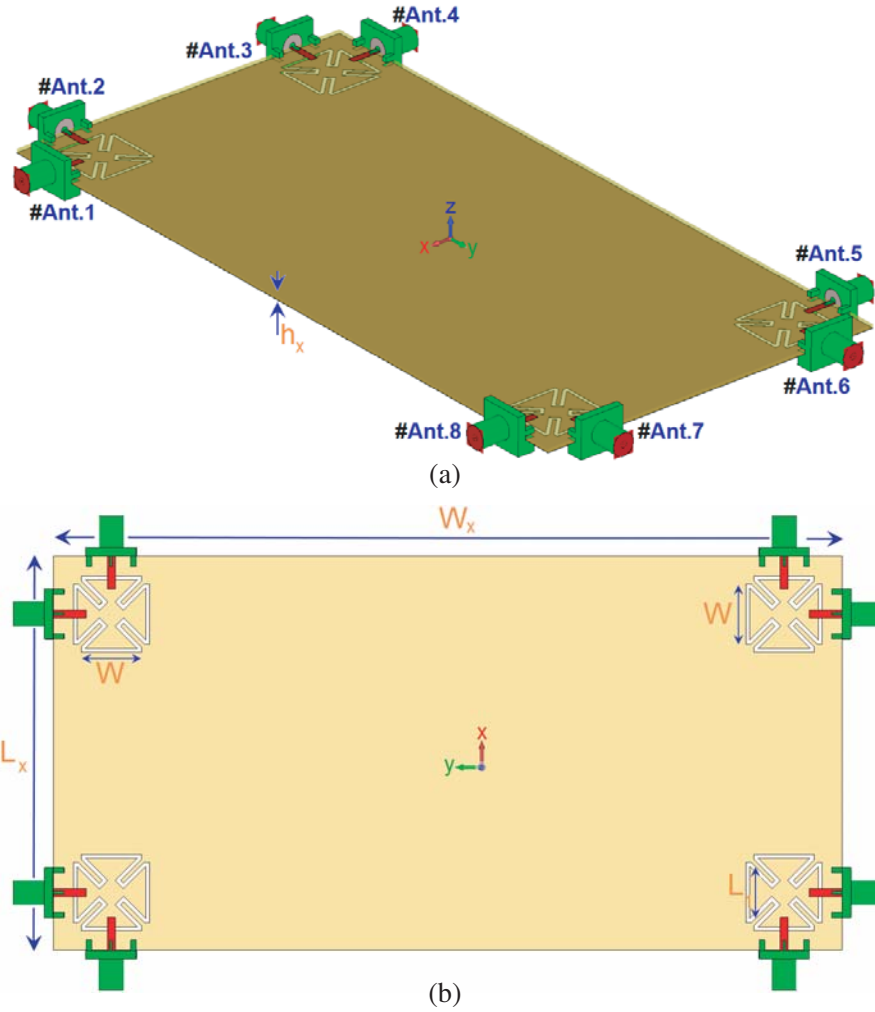
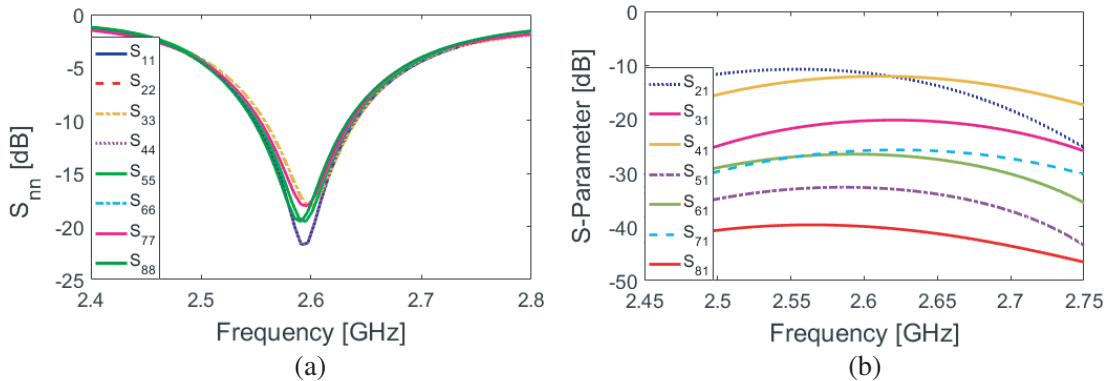


Figure 7. Measured and simulated results of the antenna  $S$ -parameters.



**Figure 8.** (a) Side and (b) top views of the design.



**Figure 9.** Simulated (a)  $S_{nn}$  and (b)  $S_{nm}$  results.

exhibits good  $S$  parameters with more than 100 MHz bandwidth and sufficient isolations (better than  $-10$  dB). Employing the petal-ring slots not only improves the impedance-matching and bandwidth of the radiators but also improves the radiation coverage of the main design to cover different regions of the main board [26]. Figure 10 depicts the 3D radiation patterns for the adjacent antenna elements (Ant. 1

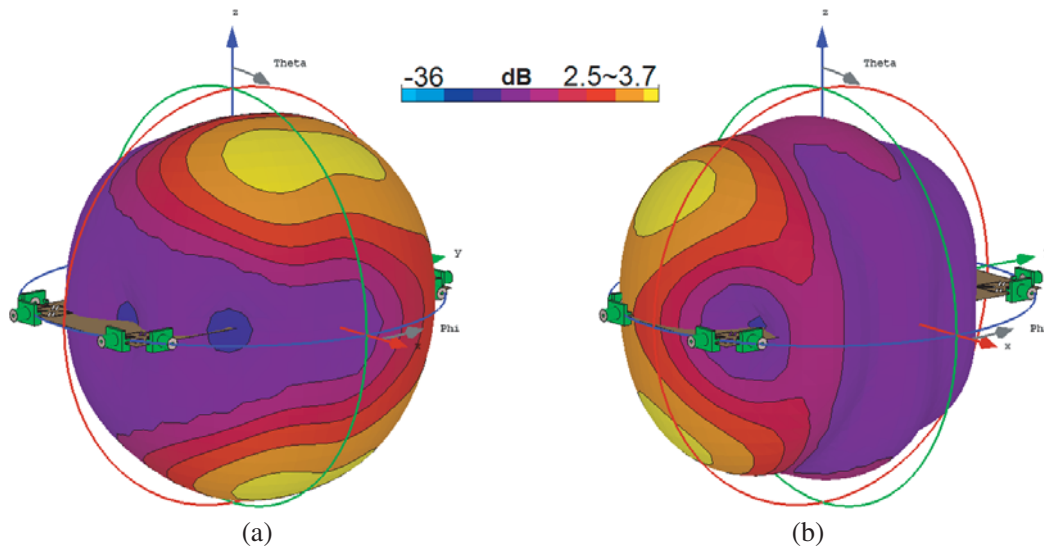


Figure 10. Radiation patterns from (a) port 1 and (b) port at 2.6 GHz.

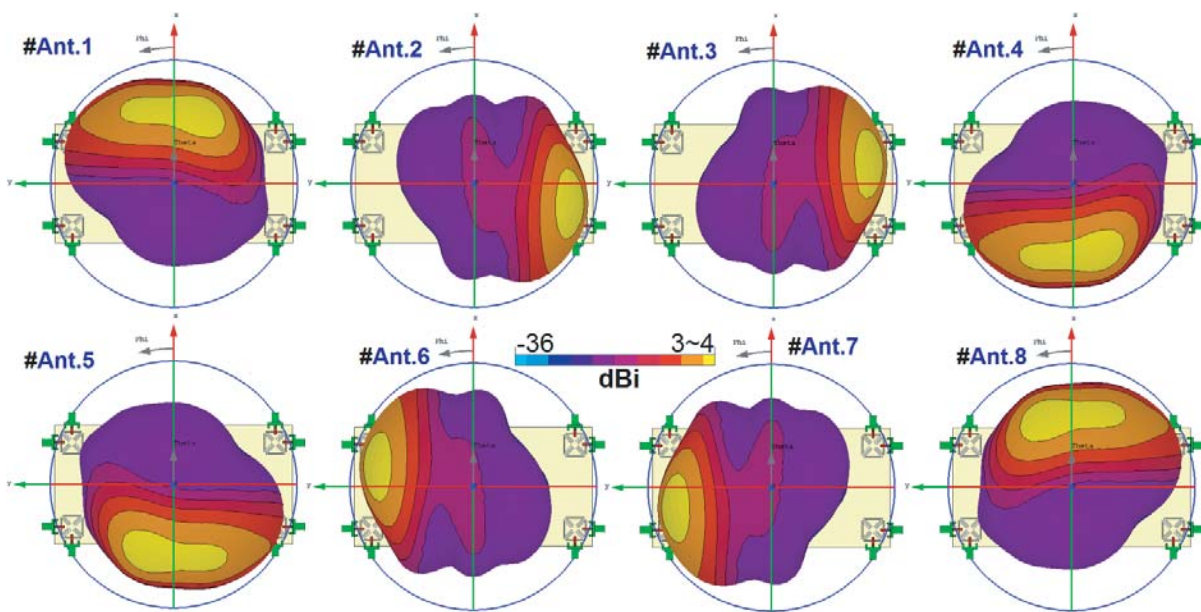


Figure 11. Simulated radiation patterns with directivity value at 2.6 GHz.

and Ant. 2). As shown, each petal-shaped slot-ring radiation element provides symmetric radiations covering the sides of the mainboard and improving the radiation coverage of the MIMO smartphone array.

The radiation patterns of the smartphone antenna array at 2.6 GHz are displayed in Figure 11. As can be observed, the 8-element MIMO antenna provides differently polarized radiation patterns for each region of pattern coverage. In other words, the proposed antenna not only can cover the required radiation pattern coverage but also provides different polarizations (horizontal/vertical) for each region of the PCB [27, 28]. Furthermore, the antenna elements provide sufficient gain levels at the resonance frequency (2.6 GHz).

The MIMO design has been fabricated, and its characteristics are examined. The front view of the prototype sample is depicted in Figure 12. Due to a similar performance of the antenna pairs, *S*-parameter results and 2D-polar patterns of the adjacent antenna elements (Ant. 1 and Ant. 2) are

measured and compared with simulations. It is evident from Figure 13 that the fabricated prototype provides good  $S$ -parameter around 2.6 GHz with sufficient frequency bandwidth and acceptable agreements with simulated design. In addition, it is seen from Figure 14 that the design exhibits good



**Figure 12.** Fabricated smartphone antenna PCB.

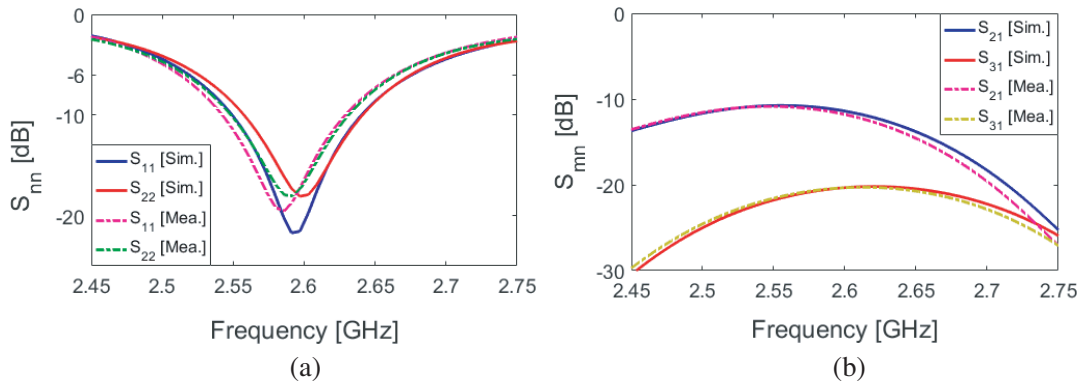


**Figure 13.** Measured and simulated (a)  $S_{nn}$  and (b)  $S_{nm}$  of the fabricated MIMO design.

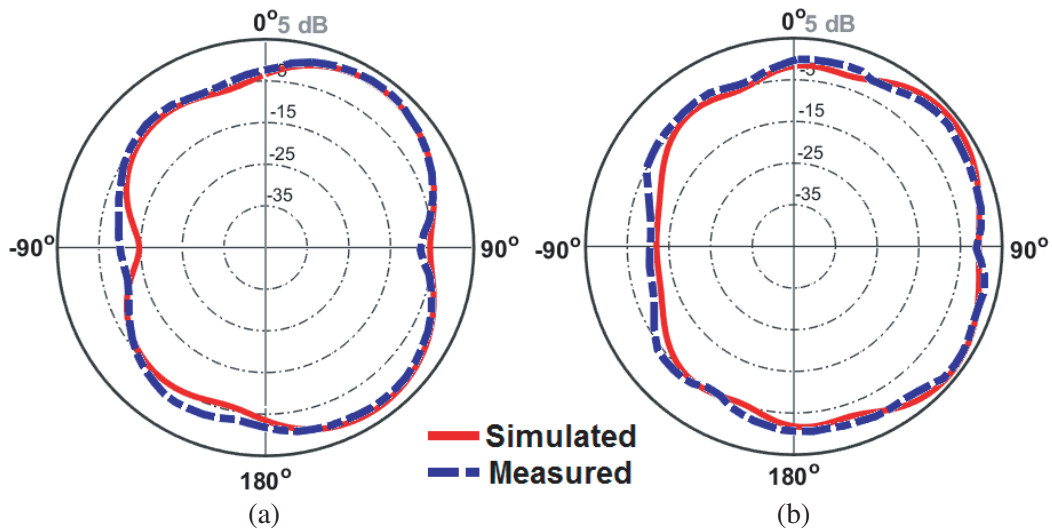


**Figure 14.** Measured and simulated radiation patterns for (a) first and (b) second elements.

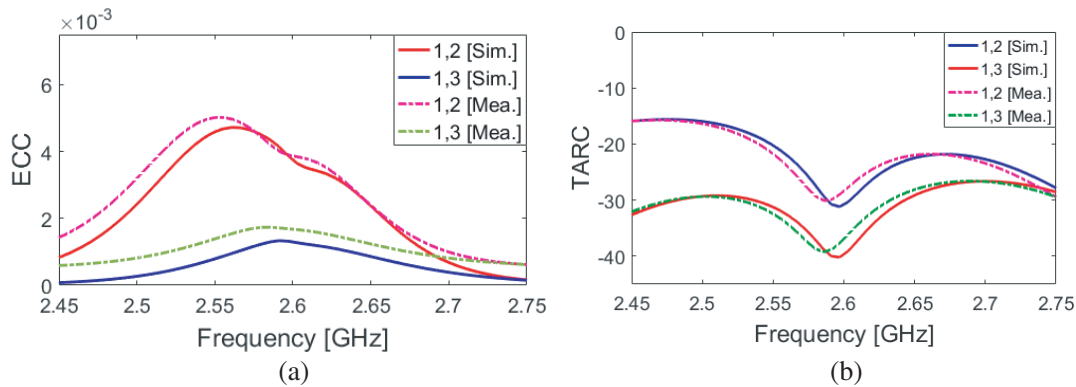
radiation patterns with quasi-omnidirectional radiation mode supporting the top and bottom sides of the substrate. Moreover, sufficient IEEE gain levels have been achieved for the antenna elements at the resonance frequency of 2.6 GHz. A slight variation in the measured  $S$ -parameters is confirmed which can be due to possible errors in fabrication and feeding.

In order to validate the capability of a MIMO antenna design, ECC and TARC properties are investigated [29, 30]. The ECC and TARC characteristics of MIMO antenna can be calculated using the formula below

$$ECC = \frac{|S_{mm}^* S_{mn} + S_{nm}^* S_{nn}|^2}{(1 - |S_{mm}|^2 - |S_{mn}|^2)(1 - |S_{nm}|^2 - |S_{nn}|^2)^*} \quad (1)$$

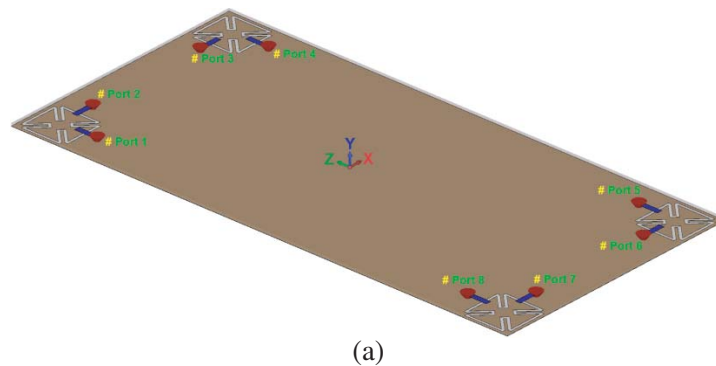
$$TARC = -\sqrt{\frac{(S_{mm} + S_{mn})^2 + (S_{nm} + S_{nn})^2}{2}} \quad (2)$$

As plotted in Figure 15(a), the calculated ECC characteristics of the MIMO design are less than 0.005. Moreover, as shown in Figure 15(b), the TARC result is less than  $-16$  dB over the entire operation band of the antenna and less than 25 dB at 2.6 GHz (the resonance frequency).



**Figure 15.** Measured and simulated (a) ECC and (b) TARC results.

In order to ease manufacturing and measurement, the antenna elements are fed and excited by coaxial SMA connectors from different edges of the smartphone mainboard. However, due to the symmetrical configuration and corner placement of the dual-polarized elements, it is possible to feed the antenna from inside the smartphone mainboard. Figure 16(a) illustrates a new arrangement of the proposed smartphone array where the main radiators are fed from inside of the PCB using the microstrip-line discrete-feeding technique. As can be seen from Figure 16(b), the smartphone antenna array provides sufficient  $S_{nn}$  results similar to the proposed array with SMA connectors with better isolation.



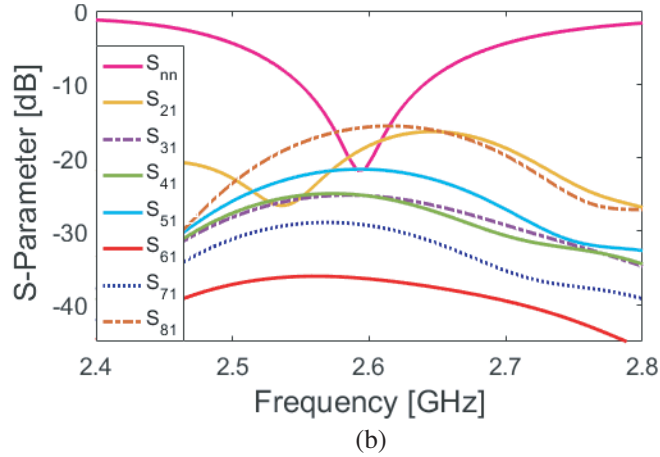


**Figure 16.** (a) Configuration and (b)  $S_{nn}$  results of the design with a different feeding arrangement.

#### 4. CONCLUSIONS

A new design of a smartphone antenna with eight radiators is introduced for 2.6 GHz mobile terminal. The configuration of the design consists of four petal-ring slot antennas placed at the corners of the smartphone board. Each petal-ring resonator is fed a pair of microstrip feeding lines and generates dual-polarized function. The MIMO system provides good radiation patterns coverage with polarization diversity function at different sides of the mainboard. Fundamental characteristics and MIMO performance of the presented design are investigated, and good results are obtained. It offers good characteristics in terms of bandwidth, isolation, and radiation pattern. A prototype sample of the design has been fabricated and examined. The proposed MIMO antenna offers good features in terms of  $S$ -parameter, antenna gain, and efficiency. It also has a planar structure and is suitable for future smartphones.

#### ACKNOWLEDGMENT

This work is supported by the European Union's Horizon 2020 research and innovation program under grant agreement H2020-MSCA-ITN-2016 SECRET-722424.

#### REFERENCES

1. Jensen, M. and J. Wallace, "A review of antennas and propagation for MIMO wireless communications," *IEEE Trans. Antennas Propag.*, Vol. 52, 2810–2824, 2004.
2. Yang, H. H. and Y. Q. S. Quel, "Massive MIMO meets small cell," *Springer Briefs in Electrical and Computer Engineering*, 2017, DOI 10.1007/978-3-319-43715-6\_2.
3. Li, M.-Y., et al., "Tri-polarized 12-antenna MIMO array for future 5G smartphone applications," *IEEE Access*, Vol. 6, 6160–6170, 2018.
4. Park, J.-D., M. Rahman, and H. N. Chen, "Isolation enhancement of wide-band MIMO array antennas utilizing resistive loading," *IEEE Access*, Vol. 7, 8120–8126, 2019.
5. Ojaroudi, N. and N. Ghadimi, "Design of CPW-fed slot antenna for MIMO system applications," *Microw. Opt. Technol. Lett.*, Vol. 56, 1278–1281, 2014.
6. Jensen, M. and J. Wallace, "A review of antennas and propagation for MIMO wireless communications," *IEEE Trans. Antennas Propag.*, Vol. 52, 2810–2824, 2004.
7. Thrane, J., et al., "Comparison of empirical and ray-tracing models for mobile Communication systems at 2.6 GHz," *2019 IEEE 90th Vehicular Technology Conference*, Honolulu, HI, USA, Sept. 22–25, 2019,

8. Li, M.-Y., et al., "Eight-port dual polarized MIMO antenna for 5G smartphone applications," *IEEE Asia Pacific Conf. on Antennas and Propagation*, 195–196, Kaohsiung, Taiwan, Jul. 26–29, 2016.
9. Nikolikj, V. and T. Janevski, "A comparative cost-capacity modeling of wireless heterogeneous networks, implemented within the 0.7 GHz, 2.6 GHz, 5 GHz and 28 GHz bands," *Proc. Int. Conf. Ultra-wideband*, 489–494, Sept. 2014.
10. Elfergani, I. T. E., et al., *Antenna Fundamentals for Legacy Mobile Applications and Beyond*, 1–659, Springer Nature, Sept. 2017.
11. Parchin, N. O., et al., "Frequency reconfigurable antenna array with compact end-fire radiators for 4G/5G mobile handsets," *IEEE 5G World Forum*, Dresden, Germany, Sept. 30–Oct. 2, 2019.
12. Sharawi, M. S., *Printed MIMO Antenna Engineering*, Artech House, Norwood, MA, USA, 2014.
13. Zhang, Z., *Antenna Design for Mobile Devices*, Wiley-IEEE Press, Hoboken, NJ, USA, 2011.
14. Ojaroudi, N., H. Ojaroudi, and N. Ghadimi, "Quad-band Planar Inverted-F Antenna (PIFA) for wireless communication systems," *Progress In Electromagnetics Research Letters*, Vol. 45, 51–56, 2014.
15. Ojaroudi, Y., et al., "Circularly polarized microstrip slot antenna with a pair of spur-shaped slits for WLAN applications," *Microw. Opt. Technol. Lett.*, Vol. 57, 756–759, 2015.
16. Zhao, X., S. P. Yeo, and L. C. Ong, "Decoupling of inverted-F antennas with high-order modes of ground plane for 5G mobile MIMO platform," *IEEE Trans. Antennas Propag.*, Vol. 66, 4485–4495, 2018.
17. Li, M.-Y., et al., "Tri-polarized 12-antenna MIMO array for future 5G smartphone applications," *IEEE Access*, Vol. 6, 6160–6170, 2018.
18. Parchin, N. O., et al., "Dual-polarized MIMO antenna array design using miniaturized self-complementary structures for 5G smartphone applications," *EuCAP Conference*, Krakow, Poland, Mar. 31–Apr. 5, 2019.
19. Abdullah, M., Y.-L. Ban, K. Kang, M.-Y. Li, and M. Amin, "Eight-element antenna array at 3.5 GHz for MIMO wireless application," *Progress In Electromagnetics Research C*, Vol. 78, 209–217, 2017.
20. *CST Microwave Studio*, ver. 2018, CST, Framingham, MA, USA, 2018.
21. Valizade, A., "Band-notch slot antenna with enhanced bandwidth by using  $\Omega$ -shaped strips protruded inside rectangular slots for UWB applications," *Appl. Comput. Electromagn. Soc. (ACES) J.*, Vol. 27, 816–822, 2012.
22. Parchin, N. O., et al., " $8 \times 8$  MIMO antenna system with coupled-fed elements for 5G handsets," *The IET Conference on Antennas and Propagation (APC)*, Birmingham, UK, Nov. 11–12, 2019.
23. Chandel, R., A. K. Gautam, and K. Rambabu, "Tapered fed compact UWB MIMO-diversity antenna with dual band-notched characteristics," *IEEE Trans. Antennas Propag.*, Vol. 66, No. 4, 1677–1684, Apr. 2018.
24. Ojaroudi, N., "Small microstrip-fed slot antenna with frequency band-stop function," *21th Telecommunications Forum, TELFOR 2013*, Belgrade, Serbia, Nov. 27–28, 2013.
25. Ojaroudi, N., "Design of microstrip antenna for 2.4/5.8 GHz RFID applications," *German Microwave Conference, GeMic 2014*, RWTH Aachen University, Germany, Mar. 10–12, 2014.
26. Sun, L., H. Feng, Y. Li, and Z. Zhang, "Compact 5G MIMO mobile phone antennas with tightly arranged orthogonal-mode pairs," *IEEE Trans. Antennas Propag.*, Vol. 66, 6364–6369, 2018.
27. Larsson, E., "Massive MIMO for next generation wireless Systems," *IEEE Commun. Mag.*, Vol. 52, 186–195, 2014.
28. Ojaroudi, N., et al., "Enhanced bandwidth of small square monopole antenna by using inverted Ushaped slot and conductor-backed plane," *Applied Computational Electromagnetics Society (ACES) Journal*, Vol. 27, No. 8, 685–690, Aug. 2012.
29. Ali, W. A. E. and A. A. Ibrahim "A compact double-sided MIMO antenna with an improved isolation for UWB applications," *AEU Int. J. Electron. Commun.*, Vol. 82, 7–13, 2017.
30. Khan, R., et al., "User influence on mobile terminal antennas: A review of challenges and potential solution for 5G antennas," *IEEE Access*, Vol. 6, 77695–77715, 2018.